RECENT PALEOENVIRONMENTAL EVOLUTION OF LAKE ISSYK-KUL

S. Giralt and J. Klerkx
Royal Museum for Central Africa (RMCA) Dept. of Geology
Leuvensesteenweg 13, B-3080 Tervuren (Belgium). e-mail: sgiralt@africamuseum.be
S. Riera
Museu, Laboratorio e Jardim Botanico de Lisboa, Laboratorio de Paleoecologia,
Rua da Escola Politecnica 58, P-1294 Lisboa (Portugal).
R. Julià
Institute of Earth Sciences "Jaume Almera" (CSIC)
Lluís Solé i Sabarís s/n, E-08028 Barcelona (Spain).
V. Lignier and C. Beck
Laboratoire de Géodynamique des Chaines Alpines, CNRS UMR 5025 - Université de Savoie, Centre Interdisciplinaire des Sciences de la Montagne
Bâtiment Belledonne - Campus Technolac, F-73376 Le Bourget du Lac Cedex.
M. De Batist
Renard Centre of Marine Geology, Geological Institute, University of Gent
Krijgslaan 281 S.8, B-9000 Gent, (Belgium).
I. Kalugin
United Institute of Geology, Geophysics and Mineralogy
Siberian Branch of Russian Academy of Sciences (UIGGM SBRAS) Laboratory of Cenozoic Geology and Paleoclimatology, Prosp. Akademika Koptyuga 3, 630090 Novosibirsk (Russia).

1. Introduction

Closed lakes located in arid and semi-arid environments are highly sensitive to climate oscillations since small variations in their environmental conditions induce dramatic changes within the lake [1]. The sensivity of these lakes is higher if they are located in the border of biomes, as Lake Issyk-Kul, located between the steppic and high mountains environments [2]. These facts make Lake Issyk-Kul an important ecosystem in order to study its adaptability under the environmental changes occurred in the Central Asia region.

The study of climatic change on prehistorical and historical timescales provides a valuable perspective for interpreting the natural trend of climatic variability of the past, and a database for assessing present and future behaviour under intensive and extensive human impacts [3].

These databases should allow the development of accurate environmental policies in order to establish a regional model for the sustainable development of the socio-economic structures, which could constitute one the basis of the economy (e.g. tourism and natural resources).

Lake Issyk-Kul constitutes one of the most important recreational resources in the Republic of Kyrgyzstan, with more than 100 recreational centres along its shore, where some 370,000 visitors stay annually [4][5], and will be higher in the near future due to the general interest in well-preserved natural environments. Thus, a careful management of this ecosystem is needed in order to promote and sustain this value.

In this paper, we present a preliminary comprehensive paleoenvironmental reconstruction of the lake evolution during the last 2000 years based on pollen and sedimentological analyses of a core 1.80 m long.

2. Site description

Lake Issyk-Kul is an endorheic mountain lake located at 1608 m a.s.l., in the northern Tien Shan ranges, in the Republic of Kyrgyzstan, Central Asia (Figure 1). It has an area of 6236 km^2, a length of 250 km, a width of 60 km, and a maximum depth of 668 m making it the fifth deepest lake in the world [6]. The lake is monomictic, saline (6 g/l), oligotrophic to ultra-oligotrophic (2 – 3.8 µg/l of phosphorous [5]), and it has high values of dissolved oxygen (6.5 – 7.5 mg/l at the bottom of the lake).

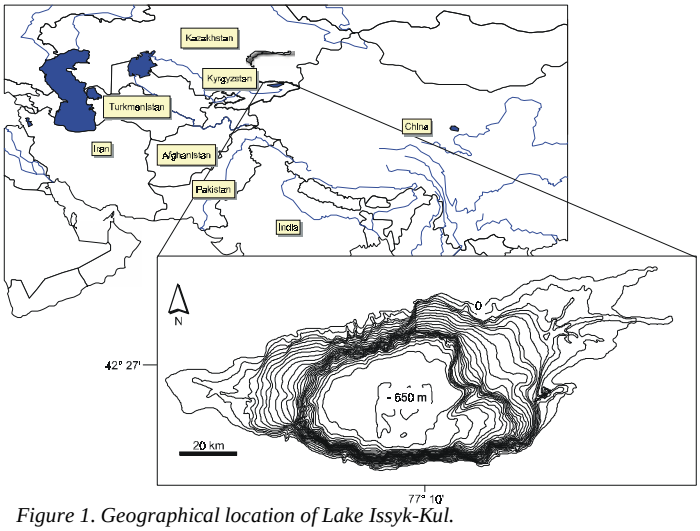

Figure 1. Geographical location of Lake Issyk-Kul.

The pH values range between 8.75, at the surface of the lake, and nearly 8 at the bottom [7]. The lake surface temperature in January is not less than 2 – 3°C, and in July it reaches 19 – 20 °C. At depths of more than 100 m, the water temperature remains constant all the year at 3.5 – 4.5 °C [8]. There are 102 streams and rivers feeding the lake. These rivers, including the two largest ones (Jergueland and Tyup rivers) are feed predominantly by meltwater from glaciers and snow, located above 3,300 m a.s.l. This fact is traduced in a mean anual oscillation of the lake level of about 20 cm (Figure 2). The lake level progressively increases from February until beginning of September, decreasing afterwards progressively to the next February.

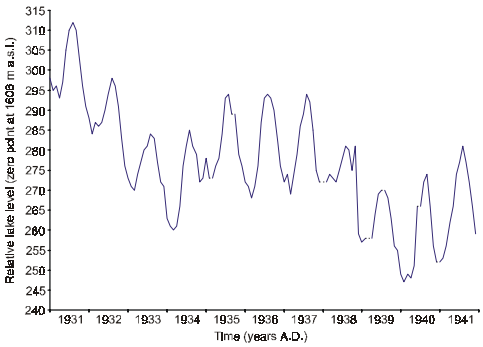

Figure 2. Monthly lake level measures for the period comprised between the years 1931 to 1941 in the town of Cholpon – Ata, located in the central northern shore of the lake.

The regional climate is highly variable from warm, temperate, and dry in the western part to slightly moist in the eastern part. Annual precipitation averages 250 mm and the annual evaporation from the surface of the lake is approximately 700 mm. The chemical water composition of the lake is dominated by sulfate among the anions and by sodium and potassium among the cations [7]. The alkalinity ranges from 310 mg/l to 330 mg/l and the calcium content is about 115 mg/l. These slight saline waters are oversaturated in calcite, monohydrocalcite and vaterite, minerals which are found in the sediments [9].

Walter and Box [10] have estudied the altitudinal belts of Northern and Central Tien Shan (Figure 3), deducing that the altitudinal distribution of vegetation belts are mainly controlled by water availability.

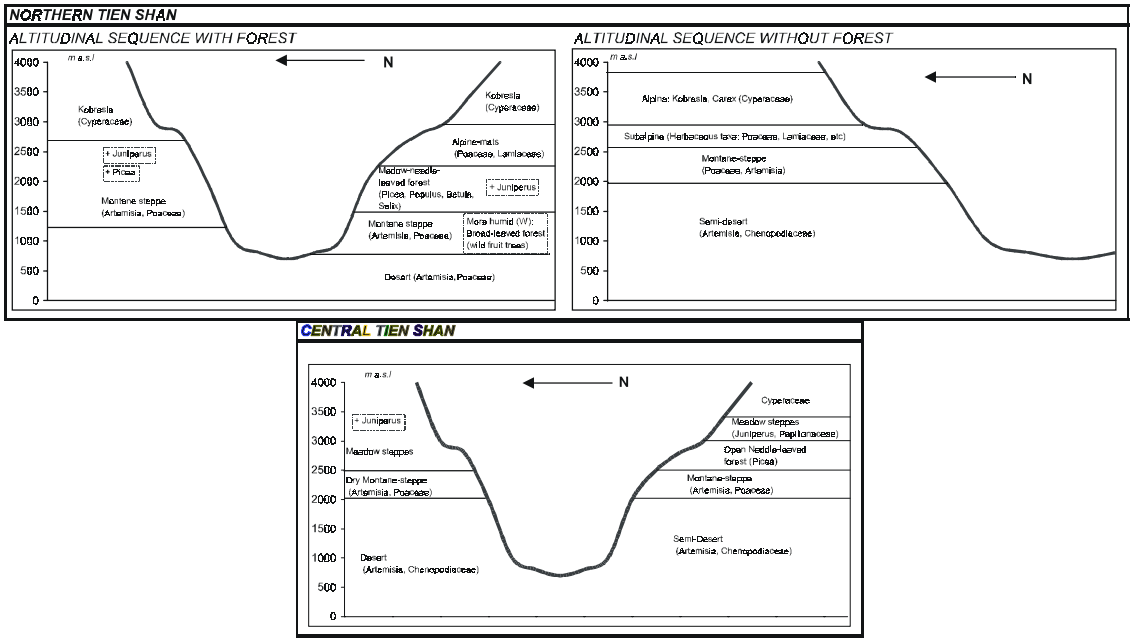

Figure 3: Altitudinal distribution of vegetation belts in Northern and Central Tien Shan ranges (modified from Walter and Box [10]).

The preliminary results of the detailed sedimentological model (seismical survey [11] and petrological studies on the recovered cores [12]) show that three main sedimentological domains have been identified [13]: 1) alternation of light and black silty-clay sediments corresponding to distal facies of deltaic lobes deposited in the eastern and western shallow shelves, apparently not affected by the regional seismicity. An interbedded coarse sandy layer in some cores from the western shelf might correspond to a debris flow, related to a punctual seismic event. 2) gravels and medium and coarse sandy sediments in a typical centimetric fining-upward sequences, corresponding to proximal turbidite facies from the apron of the deep fans, after the bypass zone of the north and south steep borders. 3) homogenous dark muddy sediments with small lenses of very fine sands of the central deep basin, corresponding either to a muddy turbidite facies (from distal mud lobes) either to an 'homogenite' facies in the sense of Sturm et al. [14]. In both cases, those sedimentary environments indicate that all these sediments are re-worked.

Thus, only the sediments present in the distal part of the shallow shelves are suitable for paleoenvironmental reconstructions. For this reason, the longest core obtained in the eastern shelf (core 98i-28) has been used for this purpose.

3. Materials and Methods

In September 1998, a coring program was conducted in Lake Issyk-Kul. Twenty-two gravity cores (maximum length was 1.80 m) and Ekman dredges were collected from the shallowest eastern part (23 m deep) to the deepest central part of the Lake (up to 668 m deep), following a longitudinal and a latitudinal transects. The core locations were based on the results of an extensive seismic survey, carried out just before the coring [11].

Dredge sediments were used for depicting the present-day sedimentary processes while the cores were used for establishing the sedimentological model that triggers the deposition processes within the lake.
All the cores were split longitudinally, and one half were wrapped in aluminum foil and stored in a cool room at +2° C for further analyses, while the other half was used for lithological description, digitalization with a CCD camera, and sampling. These cores have been subsampled and characterized using gray-scale analysis, magnetic susceptibility, granulometry, x-ray diffraction, thin sections and pollen.

The grain size analyses were conducted using a Malvern Instruments MasterSizer/E with a 2 mW He – Ne laser (633 nm wavelength). X-ray diffractions were done with an automatic Brucker D – 5005 x – ray diffractometer: Cu radiation (K_α = 1.5405), 40 kV, 30 mA and graphite monochromator. Some sediment samples were coated with carbon or gold for scanning electron microscope (SEM) observations. SEM observations were performed in a Hitachi-3000 electron microscope. The thin sections were obtained after freeze-drying and balsam hardering the samples, and a total of 100 thin sections have been studied. The thin sections were digitalized using a CCD camera, and images were used for several measurements using Scion Image software, following the technique of Francus [15]. Samples for pollen and charcoal analysis were taken every 10 centimeters. The pollen sequence has given us an overview of vegetation and environmental changes occurred in the lake basin during the late Holocene. Samples for pollen and charcoal analysis were prepared following standard procedures [16]. Lycopodium-tablets were added in order to obtain Pollen and Charcoal Concentration values (particles per gram of humid sediment). Minimum number of counted pollen per sample was established on 250 grains. Total pollen sum used for the calculation of percentage of each pollen taxa considered all pollen grains, excluding those from aquatic and semi-aquatic plants, that probably grow in the margins and the littoral part of the lake.

Concentration Particle values are mainly determined by the sedimentation rate, as we can conclude from the similar concentration evolution of both, pollen and charcoal remains (Figure 4). Due to this fact, and with the objective to remove the effect of sedimentation rate, charcoal values for paleowildfires reconstruction has been calculated as follows: Charcoal Concentration x Pollen Concentration $^{-1}$ (Figure 4).

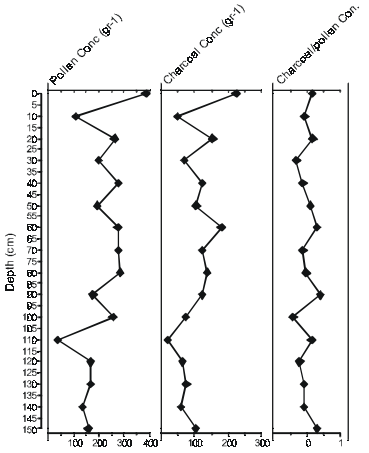

Figure 4: Pollen grains and charcoal particles concentration in the 98i-28 sequence (number of particles per gram of humid sediment).

Pollen zones were established using the Edwards and Cavalli-Sforza's chord distance of the CONISS program [17].

The degree of saturation of the lake water with respect to calcite, aragonite, monohydrocalcite, and gypsum was calculated using the computer program PHREEQCI [18][19].

The chronological framework has been established by ^{210}Pb of the 10 upper centimeters and by an AMS ^{14}C date, at 15 centimeters of depth.

4. Results

4.1 SEDIMENTOLOGICAL DESCRIPTION OF THE CORE 98I-28

The core 98i-28 has a total length of 1.80 m and it is formed by two main lithological units:
1.- The upper 15 cm are mainly formed by a massive bed of light brown silty-clays.
2.- From the 15 centimeters to the bottom of the sequence the sediments are composed by a colour alternation of light and dark gray clays. Between 0.86 m and 1.36 m of depth, the textural composition of this alternation is slightly coarser (Figure 5). Two types of colour alternation can be differentiated: a) a centimetric (1 – 2 cm thick) alternation of light and dark gray layers. The boundaries are sharp in the top of the dark lamina and transitional in the bottom of it. b) a millimetric (1 – 2 mm thick) alternation of light and dark gray lamina with clear boundaries.

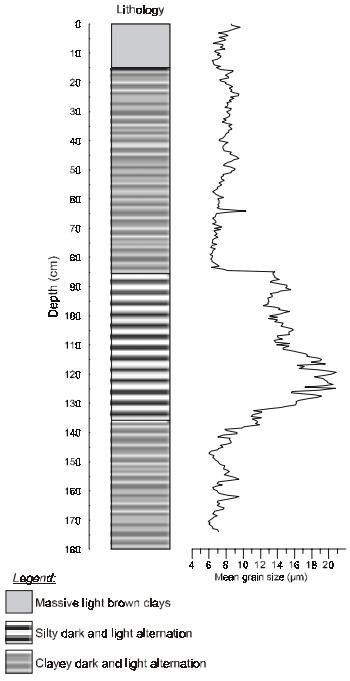

Figure 5: Main lithological units of the core 98i-28 and mean grain size of the sediments of this core.

4.1.1. Microfacies

In order to characterize this alternation, thin sections and electronic microscope observations have been performed. Three microfacies have been identified:

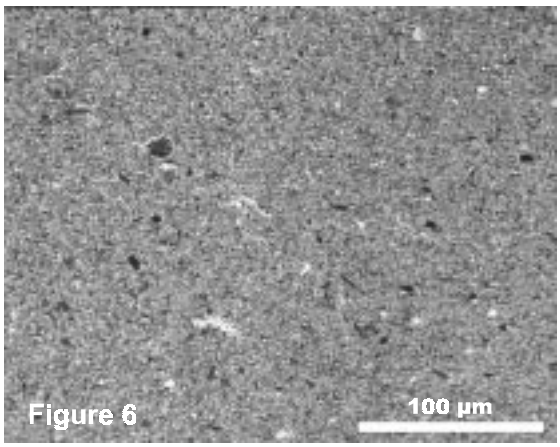

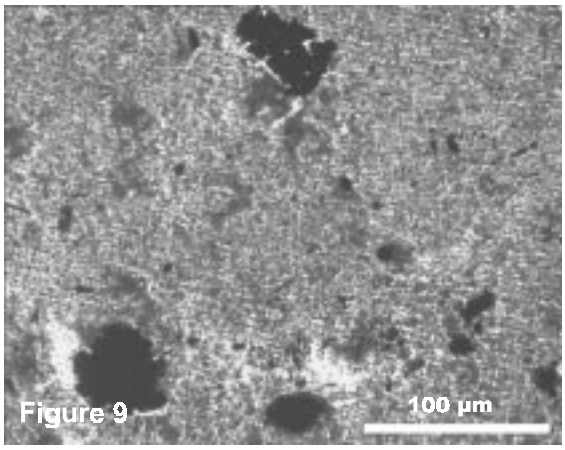

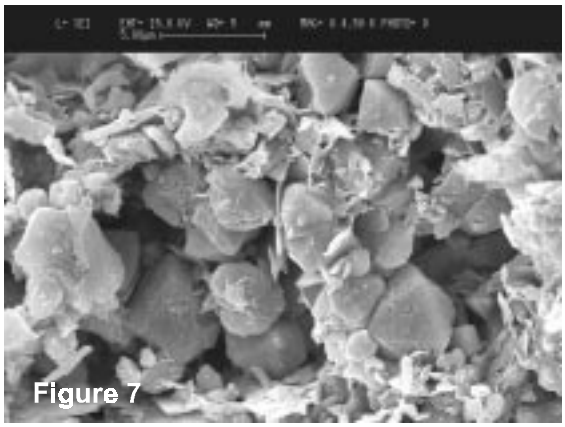

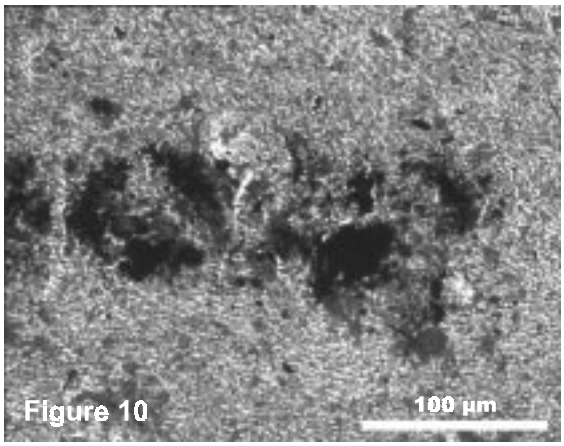

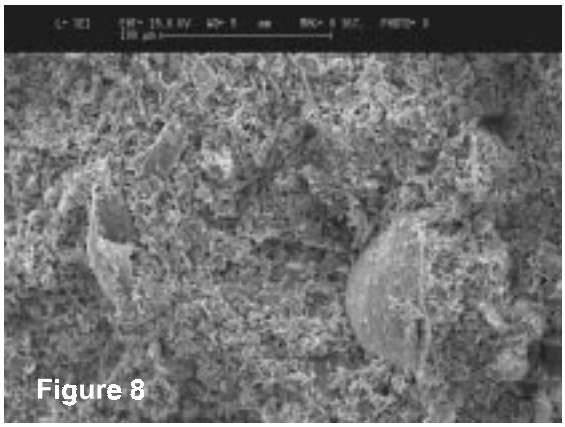

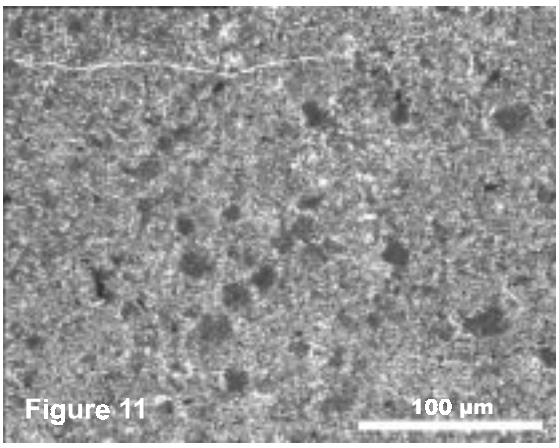

Figure 6. Common view of the microfacies 1 (82 cm of depth) in the petrographical microscope. White bar as scale.
Figure 7. Common SEM view of the crystals that compose the micrite of microfacies 1.
Figure 8. SEM aspect of the micrite composing the sediments of the core 98i-28. Note the position of the ostracode and the presence of large terrigenous particles floating in the micrite. The top of the sample is located in the left part of the photograph.
Figure 9. Common view of the dark gray lamina (99 cm of depth) at the petrographical microscope, rich in plant rests and charcoal. White bar as scale.
Figure 10. Common view of the dark gray lamina (135 cm of depth) at the petrographical microscope, rich in sulfide and/or manganese accumulations. White bar as scale.
Figure 11. Common view of the peletoidal lamina (130 cm of depth) at the petrographical microscope. White bar as scale.

Microfacies 1: light centimetric laminae The first microfacies is composed by massive micritic carbonate with some terrigenous grains floating in this matrix (Figure 6). These grains are mainly homogeneous in size and are mainly composed by quartz, hornblende and some elongated phyllosilicates, such as biotite, mainly disposed parallel to the surface of sedimentation. At the electronic microscope, this micrite is composed by euhedral and homogranular rombic crystals, with a mean size of 5 μm (Figure 7). In the other hand, the detrital grains are bigger in size an anhedral. It is also noticeable the presence of fragments of gastropods, ostracods and diatoms, most of them parallel to the surface of sedimentation (Figure 8). The preservation of the ostracods is excellent, but of the diatoms very poor. This microfacies is present from the top of the core until 85 centimeters and from 136 cm to the bottom of the core, at 180 cm of depth.

Microfacies 2: dark centimetric lamina. The second microfacies is constituted by massive micritic carbonate with large fragments of plant rests, some of them with framboidal texture, and charcoal particles (Figure 9), as well as, black masses, which could be interpreted as sulfide- and/or manganese-rich accumulations (Figure 10). These accumulations are laterally discontinuous, and their borders diffuse.

Microfacies 3: peletoidal lamina. The third microfacies is mainly composed by light massive micritic carbonate, rich in fecal pellets aggregates, with terrigenous minerals floating in this matrix, and large quantities of ostracods (complete shelves and fragments) and diatoms (Figure 11). In this case, the elongated particles are disposed without any preferential orientation. This facies dominate from 86 cm to 136 cm of depth.

4.1.2. Microfacies organization

The petrological and SEM observations suggest that the main part of the carbonates that compose these sediments are authigenic.

The facies of this core seem to correspond to a distal shelf sedimentation, affected by muddy contribution (evidenced by the terrigenous grains) related to the Jergueland and Tyup rivers, as well as to the eolian input.

These microfacies are organized forming couples of light (microfacies 1) and dark (microfacies 2) lamina. Only in the central part of the core, between 0.86 m and 1.36 m of depth, the light laminae is represented by the microfacies 3.

Origin of the millimetric alternation The ice melting, during the first half of the year, supplies large quantities of cold water, entering into the lake as interflows, over the termocline (at 30 m of water depth, approx.) and over the chemocline (at around 50 m of water depth), providing large quantities of terrigenous sediment, as well as increasing the phosphorous and iron content in the water (Figure 12). The phosphorous maximum is achieved around May, when the first algal bloom occurs [5]. This algal bloom slightly affects the carbonate precipitation, since the water of the lake remains largely supersaturated in calcite, aragonite and monohydrocalcite during all the year (Figure 12). Is during this first half of the year that the light massive lamina would form (Figure 12).

From July to March, the temperature of the water decreases, starting the overturn at the end of November. Due to the accumulation of snow in the surrounding mountains from September the river discharges decreases. This fact is traduced with the decline of the lake level. This lake level reduction, together with the decay of the Characeae, allows a relative increase of phosphorous in the water, which induces a second algal bloom, this last in October [5]. This second algal bloom also slightly affects the inorganic precipitation of carbonates (Figure 12). During the period of overturning the organic matter is incorporated to the sediments. Therefore, during this period the dark lamina would be formed.

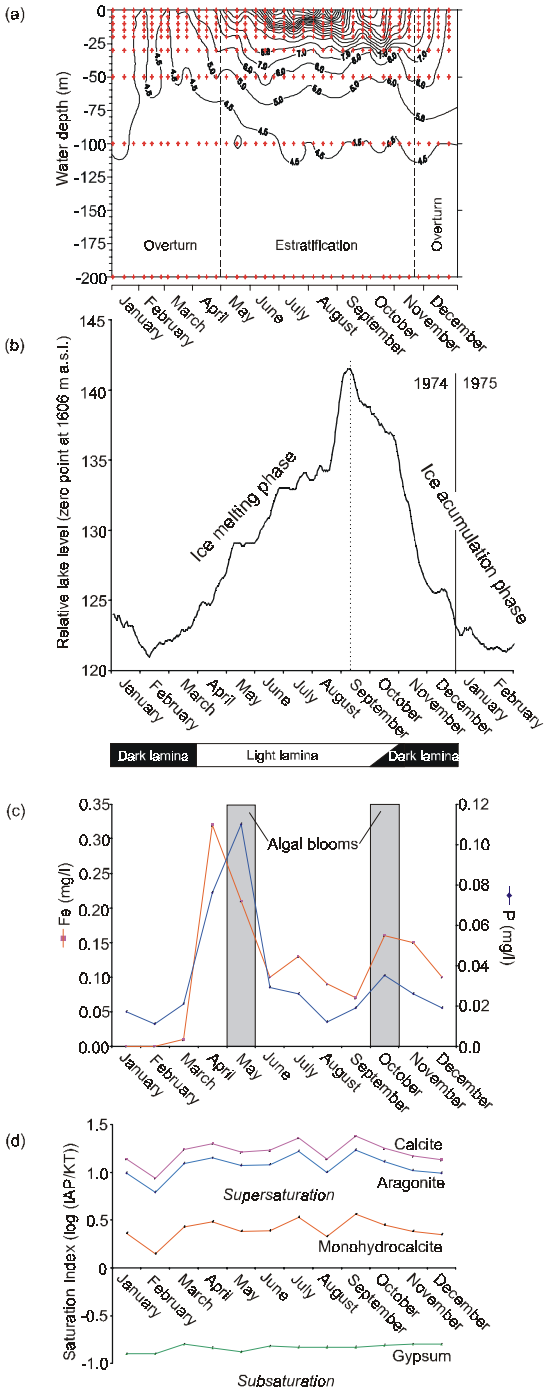

Figure 12: (a) thermal lake evolution for 1974. Note that the overturning occurs between December and April. (b) Relative daily lake level oscillation, (c) dissolved phosphorous and iron in the water, and (d) saturation indices for several carbonate species as well as for gypsum for this period.

The presence of light peloidal microfacies in the central part of the core could indicate evidences of lake dynamic changes. In fact, this facies has usually been related with shallow and low-energy inner platform

environments [20]. This fact seems to be confirmed by the large presence of rests of organisms, such as ostracods and gastropods.

Therefore, the millimetric alternation of light micritic and organic-rich facies could be interpreted in terms of rhythmites related to the ice cap melting of the surrounding mountains (Figure 12).

Origin of the centimetric alternation On the other hand, the centimetric alternation of these microfacies seems to be related to early diagenetic redox mobilization of iron associated with sulfate reduction and organic matter decay.

4.1.3. Mineralogical composition of the core 98i-28

Ten mineral species have been identified: monohydrocalcite, calcite, magnesian calcite, palygorskite, clinochlorite, quartz, illite, riebeckite, microcline and albite (Figure 13).

Carbonates compose up to 75% of the total sediment composition, and on basis of the dominance of the carbonate specie, four main zones have been established from the bottom to the top:

Zone D (180 – 147 cm deep) This zone is dominated by magnesian calcite (30 – 55%), together with rough constant values of the rest of the mineral species. In this zone illite presents its highest percentages.

Zone C (147 – 97 cm deep) Calcite dominates this zone showing percentages ranging between 50 and 75% of the total weigth. The other mineral species show the lowest values of the sequence.

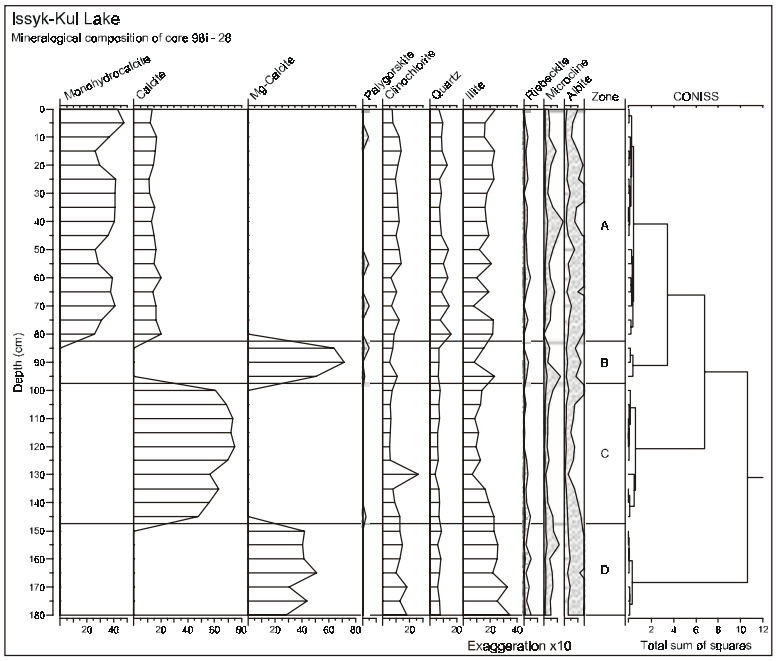

Figure 13: Mineralogical composition of the core 98i-28. Values of the different mineral species are expressed in percentage.

Zone B (97 – 83 cm deep) This zone is dominated again by magnesian calcite (50 – 72% of the total weight). It is also noticeable the near constant presence of palygorskite in this zone.

Zone A (83 – 0 cm deep) Monohydrocalcite is the main carbonate of this zone, together with a continuous presence of calcite. While the percentages of monohydrocalcite fluctuates (25 – 48% of the total weight), the percentages of calcite remain roughly constant (15%). Palygorskite is present in discrete levels and quartz shows the highest percentages of the sequence.

4.1.4. Pollen Results

With the aim to deduce and interpret the different environmental changes present in the pollen diagrams, we have grouped the different present-day pollen taxa on the basis of similar ecological requirements.

On the basis of these studies the pollen taxa have been grouped as follows (Table 1):

TABLE 1. Main ecological groups of vegetation**.**

ECOLOGY	TAXA
Desert	Chenopodiaceae, Ephedra
	Thalictrum, Caryophyllaceae
Steppe	Artemisia, Poaceae
Broad-leaved forest	Rosaceae, Acer
Needle-leaved forest	Picea, Betula, Salix
	Juniperus
Secondary Anthropic	Plantago lanceolata t.
Indicators	Plantago coronopus t.
	Rumex
Primary Anthropic	Cerealia t., Papaver
Indicators (crops)	Cannabaceae

Pollen characterization of desert and steppe vegetation has been studied with samples of modern pollen rain [21][22]. In non-forested areas of Middle East and Western Tibetian Plateau, pollen spectra are always dominated by very few taxa: *Artemisia, Chenopodiaceae, Poaceae* and *Ephedra*, while Arboreal Pollen (AP) have very low values and it usually comes from long distances. These studies show that high percentages of *Chenopodiaceae* are related with desertic conditions, while high *Artemisia* values have been recorded in more steppic conditions. The similar pollinisation mechanism of both taxa make it possible to use the relationship between *Chenopodiaceae* and *Artemisia* as an aridity index (C/A), very useful for the palaeoecological and palaeoclimatic interpretation of pollen sequences located in the desert-steppe limit [23]. This index has been also applied to the Lake Issyk-Kul sequence (Figures 14 and 15).

The use of *Poaceae* as palaeoclimatic indicator is less clear. Several authors interpreted that grassland increase in these environments as a signal of moister conditions [22][24], mainly of summer rainfall increase [24]. However, *Poaceae* can be also produced by wetland vegetation and then its variations could be related with changes in lake margins and water level. In these cases, an increase of *Poaceae* could be due to a decrease in the lake water level and so, it can be interpreted as a result of drier conditions [22].

The Lake Issyk-Kul pollen diagram is mainly characterized by the absolute dominance of Non-Arboreal Pollen (NAP). Arboreal Pollen (AP) averages along the sequence is 6.5%, with highest values of 12.2% and lowest ones of 3.5%. Mean values of NAP are about 90%. Inside the AP group, *Picea* is the best represented taxon, with mean values of 2.1%. NAP group is mainly represented by *Artemisia*, with mean values of 58% and maximum of 67%, *Chenopodiaceae* (mean values of 16% and maximum of 23.6%), *Poaceae* (with mean values of 10%), *Cyperaceae* (mean values of 2.5%) and *Ephedra* (mean of 2%).

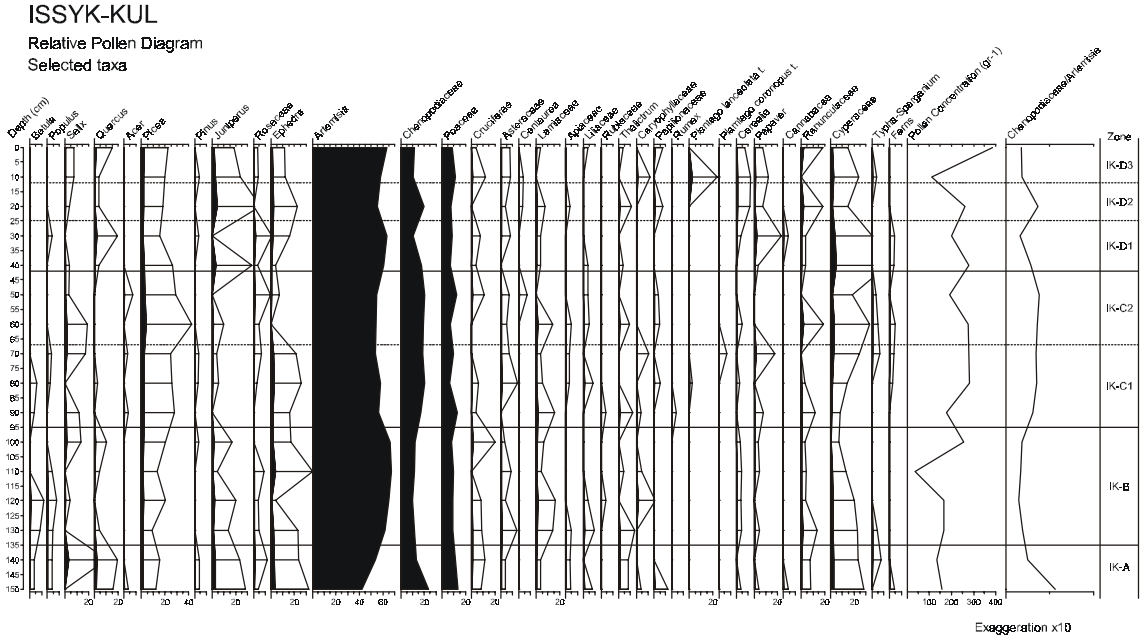

Figure 14: Relative pollen diagram of the core 98i-28. The values of the different taxa are represented in percentage.

On the basis of the CONISS results, four main pollen zones from the bottom to the top of the sequence have been established:

IK-A (150-135 cm) Besides of the high *Artemisia* pollen percentages, this zone is characterized by high values of *Chenopodiaceae* (c. 20%), Poaceae (15%), *Ephedra* and semi-aquatic herbs (*Cyperaceae*, *Typha-Sparganium* and Ferns). The synthetic pollen diagram (Figure 14) also shows the development of the desert and the retraction of steppe communities. The expansion of AP at this moment (mainly *Salix*, *Quercus*, *Juniperus* and *Rosaceae*) can be a statistical artifact resulting from the low *Artemisia* representation, because this plant produces and diperses great amounts of pollen. Pollen and Charcoal Concentration values are low in this zone and in the next one, as a result of high sedimentation rate (Figure 4).
This pollen spectrum together with the high values of the aridity index (C/A) indicate a period of dry conditions and low lacustrine water level (Figure 14).

IK-B (135-95 cm) First major change in pollen spectra occurs at 135 cm depth. Now, *Artemisia* values increase (65%) while *Chenopodiaceae* decreases (10%). The reduction of semi-aquatic herbs is progressive and this group attains its lower values later, during the transition between zones IK-B and IK-C. The aridity index C/A is very low. All this data allow us to point out a period of expansion of steppe and retraction of desert, that means an increase in regional humidity, which preludes a later water lake raising. Lower AP relative values must be seen as the result of the increase of anemophilous taxa, such as *Artemisia.*

IK-C (95-42 cm) Main pollen changes are related with the decrease of *Artemisia* pollen (55%) and the increase of desertic taxa (mainly *Chenopodiaceae* and *Ephedra* in subzone IK-C1). The increase of C/A index shows the establishment of drier conditions. However, semi-aquatic plants react later to this environmental change, and the subsequent decrease in water lake level occurs during zone IK-C2. Important changes occurred in the arboreal vegetation: *Juniperus* forest reduces and *Picea* expands at the same moment that broad-leaved forest (mainly formed by *Rosaceae*) develops. During this zone appears

the first signals of anthropogenic activity in the region, pointed out by the first important peak of *Papaver* during zone C1 as well as by the expansion of the secondary anthropogenic indicators (*Plantago sp.* and *Rumex*).

The increase of Pollen Concentration can be interpreted as a decrease in the sedimentation rate, a tendency that will continue during most part of the zone IK-D.

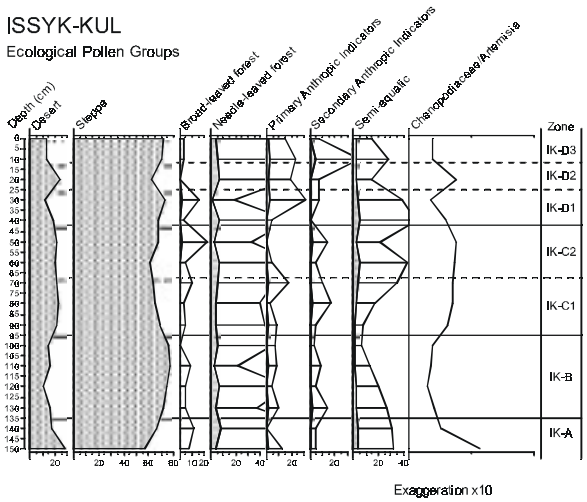

Figure 15: Ecological pollen groups established according to the classification of Walter and Box [10]. See Table 1 for the detailed composition of these groups.

IK-D (42-0 cm) This zone is mainly characterized by the expansion of primary and secondary anthropogenic indicators related to grazing and farming activities. This fact suggests that the anthropic management of the territory plays now an important role in the landscape morphology. *Cereal* and *Papaver* crops expand now around the lake, mainly during the sub-zone IK-D1.

During this zone, and related with the configuration of forests of Tien Shan slopes, *Picea* and broad-leaved forests decrease while *Juniperus* (a tree growing at higher altitude) expands (Figure 3). This forest dynamic implies an altitudinal lowering of the vegetational mountain belts towards the plains, suggesting a new climatic deterioration or man deforestation in the highest parts of the mountains.

New climatic shifts can be also observed. During the zone IK-D1, *Artemisia* develops as a result of a new increase in the moister conditions, as can be observed from the decrease of the C/A aridity index. In spite of this, higher values of semi-aquatic plants occur at the same moment showing low lake levels related to the previous aridity maximum of zone IK-C2. In the subzone D2, a new expansion of desert taxa occurs (*Chenopodiaceae, Ephedra*) showing the prevalence of dry climatic conditions during a short period of time. This short climatic deterioration could be also related to changes in the forest belts of the Tien Shan ranges (broad-leaved forest disappears and *Picea* communities reduce at the same moment that *Juniperus* develops at higher altitudes).

During the last subzone IK-D3, regional climatic moisture increases as can be deduced from high values of *Artemisia*. The reduction of desert taxa (*Ephedra, Chenopodiaceae*), the decrease of C/A index, and the low values of semi-aquatic plants can be also related with a water lake rise. This sub-zone is mainly characterized by the increase of secondary anthropogenic indicators showing again the intensification of human activities (mainly grazing), and by the increase of Pollen Concentration as a result of a low sedimentation rate.

5. Discussion

5.1. POLLEN DISCUSSION

Changes in pollen sequences entirely dominated by non-arboreal elements (NAP) are difficult to interpret in terms of environmental and/or climatic changes.

Globally, this pollen spectra allow us to establish a good relation between the Lake Issyk-Kul pollen diagram and those coming from several lakes studied in Central Asia, such as Sumxi Co [25] and Bangong Co, in Western Tibetian Plateau [22], or Mans Lake, in Northern Xinjiang [23]. However, in these lakes, AP values (average of c. 2%) are always lower than in Lake Issyk-Kul (6.5%). Pollen sequences from the west (e.g. Caspian Sea) show a diverse spectra, mainly dominated by *Chenopodiaceae*, with low *Artemisia* percentages and with higher percentages of AP (c. 20%) [26].

5.1.1. Temporal framework

The chronological framework of the sequences has been established using two approaches:

The first approach has been carried out for the upper 15 cm of the sequence, where the ^{210}Pb profile and the AMS ^{14}C radiometric date has been used. A plant macrorest located at 15 cm of depth gave an uncalibrated age of 990 ±40 years B.P.

The profile of ^{210}Pb for the upper 10 cm of sequence shows the typical exponential decay with depth (Bobrov comm. pers.). The ^{210}Pb values are roughly constant at 8 cm of depth, which means an age of 150 – 200 years at this depth. Thus, the sedimentation rate deduced from the first method is 0.5 ± 0.05 mm per year.

The sedimentation rate calculated from the second method is 0.15 mm per year. The dated plant remain was recovered from the contact between the two main lithological units. This fact, together with the disagreement with the ^{210}Pb sedimentation rate suggest that this plant remain could have a detrital origin, giving an older date.

Thus, the lack of reliable material suitable for radiocarbonic dating has not allowed to perform this technique. Then, the second approach has been applied, and a preliminary chronological framework for the rest of the sequence has been established using the lamination. Assuming the annual character of the millimetric rythmytes (as can be deduced from the annual lake limnological evolution represented in Figure 12) it has been measured the mean thickness of a couple of lamina in several parts of the core. The mean thickness is about 0.1 cm, which means a sedimentation rate of about 1mm per year. This calculated sedimentation rate is in accordance with this deduced from the ^{210}Pb method.

Taking into account this hypothetical sedimentation rate the sequence only seems to record the late Holocene, may be as far as 2,000 years. The continuous presence of crop taxa in the pollen diagram also suggests a late Holocene age.

5.1.2. Lake evolution

The total amount of carbonate throughout the Lake Issyk-Kul sequence is around 53% in average. This fact implies that the carbonate production within the lake has been roughly constant during the late Holocene. Changes in the predominant carbonate specie indicates variations in the lacustrine dynamic.

The lower part of the core is characterized by the alternation of calcite and magnesian calcite, indicating changes in salinity in the lake water, from saline conditions towards to more fresh water to, again, more saline waters (Figure 16). But, the main change in the mineralogical diagram is present at 0.85 m of depth when appears monohydrocalcite.

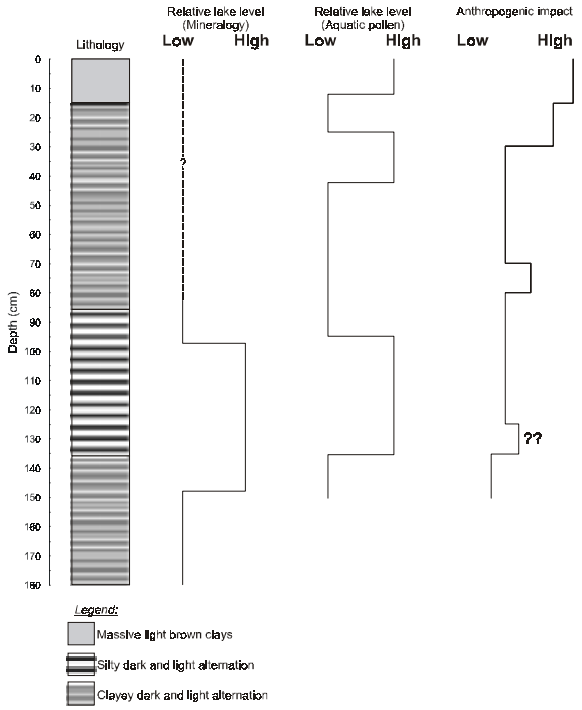

Figure 16: Lake level oscillations inferred from mineralogical composition and percentages of aquatic pollen, and compared with the anthropogenic impact on the surroundings of the lake.

The environmental conditions for the precipitation of this hydrated carbonate in natural conditions have been not yet precisely established, although it has been described in several lakes, such as as Lake Fellmongery, in South Australia [27][28] and Lake Kivu, in East Africa [29].

Several thermodynamic constants from monohydrocalcite have been accurately determined [30][31]. These studies have shown that this carbonate mineral specie belongs to a solid phase solution, which progressively increases its stability (ikaite < monohydrocalcite < vaterite < aragonite < calcite). Ikaite and monohydrocalcite usually convert to vaterite and to calcite, which are more stable carbonate forms.

It seems that, in experimental conditions, three main factors control the precipitation of these hydrated carbonates:

1.- the salinity: high Mg/Ca ratios inhibite the formation of calcite [32][33][34] and favours both the precipitation of high-magnesian carbonates, such as magnesian calcite and dolomite, among others [35][36], and of hydrated carbonates, as monohydrocalcite [37][28].

2.- the presence of phosphate: several works have demonstrated that the presence of phosphorous in the water (as sodium hexametaphoshate or triphosphate) inhibites the spontaneous precipitation of anhydrous carbonates, even they are supersaturated, and stabilizes the hydrated forms (such as the monohydrocalcite, ikaite or nesquehonite) [38][30][29][39][40][41]. It seems that the phosphate tends to be absorbed on the surface of the nuclei of calcite whose growth is thus inhibited [37]. Bischoff et al. [41] have reported that ikaite crystals persisted during 160 days in Walker Lake waters, just adding 100 μm of KH_2PO_4 solution.

3.- the water temperature: the hydrated carbonates seem to be “stabilized” at low water temperatures (in the case of ikaite, this mineral specie precipitates when the temperature of the water is close to 0 °C). The experiments carried out by Stoffers and Fischbeck [29] demonstrated that the precipitation of monohydrocalcite is favoured by low temperatures (around +2 °C). These mineral species became unstable with the progressive increase of the water temperature, changing to a more stable carbonate species, such as calcite. This temperature dependence seems to be overcomed by the presence of phosphate in the water [40][41].

Thus, the presence of monohydrocalcite in Lake Issyk-Kul can be interpreted as an increase of phosphorous in the lake water. This increase could be related to the closure of the output of the lake. This closure could be caused due to both tectonic activity and to increasing dryness. Bondarev and Sevastyanov [42] suggest that the tectonic activity led to changes in the flow of the Chu river and its separation of the lake. This activity seemed to be important during the end of the Late Pleistocene, but not during the Holocene. These authors also suggest that during the last 10,000 years the lake level oscillations seemed to be mainly triggered by changes in moisture.

In any case, both processes implies a reduction of the lake water volume, increasing the phosphorous concentration present in the water. This lake level decrease is visible in the western and southern part of the lake, where recent lacustrine sediments outcrop.

A third factor that could let an increase of phosphorous in the water of the lake is the anthropogenic activity in the shores of the lake. In fact, the beginning of the monohydrocalcite formation broadly coincides with the first signals of anthropic management of the territory (clearly pointed out by the presence of crop taxa such as *Plantago sp.* and the first important expansion of *Papaver*). According to the preliminary chronological framework this change took place around the 1100 A.D.

Since then, this anthropic activity has becomed progressively more important towards the present-day.

There are no clear evidences in order to descipher which factor provocated the increase of phosphorous in the lake waters, but the increase of values of aquatic taxa during this moment (Figure 16) seems to indicate that the phosphorous increase was due to natural causes (climatic and /or tectonic) rather than due to human activities. These last ones, if they have affected the lake, seems that they only have had acted amplifying this phenomena.

Although the lake level has changed during this last period, the phosphorous concentration in the water has remained high enough for favouring the precipitation of monohydrocalcite until the present-day.

6. References:

[1] Fritz, S. C. (1996) Paleolimnological records of climatic change in North America. *Limnology and Oceanography* **41**, 882 – 889.

[2] Walter, H. (1977) *Zonas de vegetación y clima*. Ediciones Omega, Barcelona.

[3] Feng, Z., Thompson, L.G., Mosley-Thompson, E. and Yao, T. (1996) Temporal and spatial variations of climate in China during the last 10 000 years. *The Holocene* **3**, 174 – 180.

[4] Romanovsky, V.V. (1990) *Lake Issyk-Kul – a natural system.* Ilim., Frunze, 168 pp.

[5] Savvaitova, K. and Petr, T. (1992) Lake Issyk-Kul, Kirgizia. *International Journal of Salt Lake Research* **1**, 21 - 46.

[6] Sevastyanov, D.V., Mamedov, E.D. and Rumyantsev, V.A. (Eds) (1991) *History of Lakes Sevan, Issyk-Kul, Balkhash, Zaisan and Aral.* Nauka, Leningrad. (in Russian).

[7] Sapozhnikov, D.G. and Viselkina, M.A. (1960) *Recent sediments of the Lake Issyk-Kul and its bays.* Publ. House Akademii Nauk, Moscow. (in Russian).

[8] Aladin, N.V. and Plotnikov, I.S. (1993) Large saline lakes of former USSR: a summary review, *Hydrobiologia* **267**, 1-12.

[9] Giralt, S., Julià, R. and Klerkx, J. (2001) Microbial biscuits of vaterite in Lake Issyk-Kul (Republic of Kyrgyzstan). *Journal of Sedimentary Research* **71** (3).

[10] Walter, H. and Box, E.O. (1983) The orobiomes of Middle Asia. In: West, N.E. (Ed.) *Ecosystems of the world: temperate deserts and semi-deserts*. Elsevier scientific publishing company, Amsterdam.

[11] Imbo, Y., De Batist, M., Klerkx, J., Lignier, V., Giralt, S., Vermeesch, P. and Beck, C. (1999) High-resolution reflection seismic study of the sedimentary infill of Lake Issyk-Kul, Kirghyzstan, Central Asia. Lennou Conference, Brest.

[12] Giralt, S., Lignier, V., Klerkx, J., Julià, R., De Batist, M., Beck, C. y Kalugin, I. (2000) Sedimentological processes in Lake Issyk-Kul (Republic of Kyrgyzstan, Central Asia): the importance of tectonically influenced sedimentation. 8th International Symposium on Paleolimnology. Kingston, Canada.
[13] Giralt, S., Lignier, V., Klerkx, J., Beck, C., Kalugin, I. and De Batist, M. (in preparation) General sedimentary pattern in Lake Issyk-Kul (Republic of Kyrgyzstan). Sedimentology.
[14] Sturm, M., Siegentahler, C. and Pickrill, R.A. (1995) Turbidites and 'homogenites'. A conceptual model of flood and slide deposits. *Publ. IAS – 16th Regional Meeting Sedimentology* **22**, 140.
[15] Francus, P. (1998) An image-analysis technique to measure grain-size variation in thin sections of soft clastic sediments. *Sedimentary Geology* **121**, 289 – 298.
[16] Moore, P.D., Webb, J.A. and Collinson, M.E. (1991) *Pollen analysis*, Blackwell scientific publications, Oxford.
[17] Grimm, E.C. (1987) Coniss: A Fortran 77 Program for Stratigraphically Constrained Cluster Analysis by the Method of Incremental Sum of Squares. *Computers & Geosciences* **13**, 13 – 35.
[18] Parkhurst, D.L. (1995) User's guide to PHREEQC − a computer program for speciation, reaction-path, advective-transport, and inverse geochemical calculations. *U.S. Geological Survey. Water-Resources Investigations Report* **95 – 4227**. 143 pp.
[19] Charlton, S.R., Macklin, C.L. and Parkhurst, D.L. 1997. PHREEQCI – a graphical user interface for the geochemical computer program PHREEQC. *U.S. Geological Survey. Water-Resources Investigations Report* **97 – 4222**, 9.
[20] Wright, V.P. and Burchette, T.P. (1996) Shallow-water carbonate environments. In: Reading, H.G. (Ed.) *Sedimentary environments: processes, facies and stratigraphy*. Blackwell science, Oxford, 325 – 394.
[21] El-Moslimany, A.P. (1990) Ecological significance of common non-arboreal pollen: examples from drylands of the Middle East. *Review of Paleobotany and Palynology* **64**, 343 – 350.
[22] Van Campo, E., Cour, P. and Sixuan, H. (1996) Holocene environmental changes in Bangong Co basin (western Tibet). Part 2: the pollen record. *Palaeogeogr., Palaeoclim., Palaeoecol.* **120,** 49 – 63.
[23] Rhodes, T.E., Gasse, F., Ruifern, L., Fontes, J.C., Keqin, W., Bertrand, P., Gibert, E., Mélières, F., Tucholka, P., Zhixiang, W. and Zhi-Yuan, C. (1996) Late Pleistocene – Holocene lacustrine record from Lake Manas, Zunggar (northern Xinjiang, Western China). *Palaeogeogr., Palaeoclim., Palaeoecol.* **120**, 105 – 121.
[24] Zang, H.C., Ma, Y.Z., Wünnemann, B. and Pachur, H.J. (2000) A Holocene climatic record from arid northwestern China. *Palaeogeogr., Palaeoclim., Palaeoecol.* **162**, 389 – 401.
[25] Van Campo, E. and Gasse, E. (1993) Pollen- and diatom-inferred climatic and hydrological changes in Sumxi Co basin (Western Tibet) since 13,000 yr B.P. *Quaternary Research* **39**, 300 – 313.
[26] Leroy, S.A.G., Marret, F., Chalié, F. and Gasse, F. (2000) Understanding the Caspian Sea erratic fluctuations: palynological results from the south basin. *Terra Nostra* **2000/7**, 45 – 49.
[27] Taylor, G.F. (1975) The occurrence of monohydrocalcite in two small lakes in the south-east of South Australia. *American Mineralogist* **60**, 690 – 697.
[28] Davies, P.J., Bubela, B. and Ferguson, J. (1977) Simulation of carbonate diagenetic processes: formation of dolomite, huntite and monohydrocalcite by the reactions between nesquehonite and brine. *Chemical Geology* **19**, 187 – 214.
[29] Stoffers, P. and Fischbeck, R. (1974) Monohydrocalcite in the sediments of Lake Kivu (East Africa). *Sedimentology* **21**, 163 – 170.
[30] Hull, H. and Turnbull, A.J. (1973) A thermodynamical study of monohydrocalcite. *Geochimica et Cosmochimica Acta* **37**, 685 – 694.
[31] Königsberger, E., Königsberger, L.C. and Gamsjäger, H. (1999) Low-temperature thermodynamic model for the system Na_2CO_3 – $MgCO_3$ – $CaCO_3$ – H_2O. *Geochimica et Cosmochimica Acta* **63**, 3105 - 3119.
[32] McConnell, J.D.C. (1960) Vaterite from Ballycraigy, Larne, Northern Ireland. *Mineralogical Magazine* **32**, 535 – 545.
[33] Reddy, M.M. (1986) Effect of magnesium ions on calcium carbonate nucleation and crystal growth in dilute aqueous solutions at 25 °C. In: Mumpton, F.A. (Ed) Studies in diagenesis. *U.S. Geological Survey Bulletin* **1578**, 169 – 182.
[34] Sawada, K. 1997. The mechanisms of crystallization and transformation of calcium carbonates: *Pure and Applied Chemistry* **69**, 921 - 928.
[35] Folk, R.L. Land, L.S. (1975) Mg/Ca Ratio and Salinity: Two Controls over Crystallization of Dolomite. *The American Association of Petroleum Geologists*: 60 – 68.
[36] Last, W. M. and De Deckker, P. (1990) Modern and Holocene carbonate sedimentology of two saline volcanic maar lakes, southern Australia. *Sedimentology* **37**, 967 – 981.
[37] Lippmann, F. (1973) *Sedimentary Carbonate Minerals*. Springer-Verlag, Berlin.
[38] Marschner, H. (1969) Hydrocalcite ($CaCO_3 \cdot H_2O$) and nesquehonite ($MgCO_3 \cdot 3H_2O$) in carbonate scales. *Science* **165**, 1119 – 1121.
[39] Shaikh, A.M. and Shearman, D.J. (1986) On ikaite and the morphology of its pseudomorphs. In: Rodríguez-Clemente, R. and Tardy, Y. (Eds) *Geochemistry and mineral formation in the earth surface*. Proceedings of the International Meeting "Geochemistry of the earth surface and processes of mineral formation", 791 – 803.
[40] Clarkson, J.R., Price, T.J. and Adams, C.J. (1992) Role of metastable phases in the spontaneous precipitation of calcium carbonate. *Journal of Chemical Society, Faraday Trans.* **88**, 243 – 249.
[41] Bischoff, J.L., Fitzpatrick, J.A. and Rosenbauer, R.J. (1993) The solubility and stabilization of ikaite ($CaCO_3.6H_2O$) from 0° to 25 °C: environmental and paleoclimatic implications for thinolite tufa. *The Journal of Geology* **101**, 21-33.
[42] Bondarev, L.G. and Sevastyanov, D.V. (1991) *The history of Sevan, Issyk-Kul, Balkhash, Zaisan and Aral Lakes*, Nauka, Leningrad. (In Russian).